JACS
JOURNAL OF THE AMERICAN CHEMICAL SOCIETY

Article

pubs.acs.org/JACS

Activities and Stabilities of Au-Modified Stepped-Pt Single-Crystal Electrodes as Model Cathode Catalysts in Polymer Electrolyte Fuel Cells

Kensaku Kodama,* Ryosuke Jinnouchi, Naoko Takahashi, Hajime Murata, and Yu Morimoto

Toyota Central R&D Laboratories, Inc. 41-1 Yokomichi, Nagakute, Aichi 480-1192, Japan

Supporting Information

ABSTRACT: The purpose of this study is to test the concept of protecting vulnerable sites on cathode catalysts in polymer electrolyte fuel cells. Pt single-crystal surfaces were modified by depositing Au atoms selectively on (100) step sites and their electrocatalytic activities for oxygen reduction reaction (ORR) and stabilities against potential cycles were examined. The ORR activities were raised by 70% by the Au modifications, and this rise in the activity was ascribed to enhanced local ORR activities on Pt(111) terraces by the surface Au atoms. The Au modifications also stabilized the Pt surfaces against potential cycles by protecting the low-coordinated (100) step sites from surface reorganizations. Thus, the surface modification by selective Au depositions on vulnerable sites is a promising method to enhance both the ORR activity and durability of the catalysts.

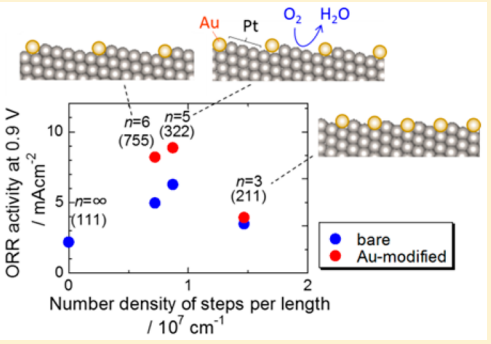

INTRODUCTION

The energy conversion efficiency of polymer electrolyte fuel cells (PEFCs) is most strongly influenced by the catalytic activities for oxygen reduction reaction (ORR) in the cathode. Platinum is the best single-metal catalyst, giving a high specific activity for ORR (activity per surface area of the catalyst surface),[1,2] and in its practical applications, Pt nanoparticles with a diameter of 2−3 nm supported on high-surface-area carbons are used to utilize a high mass activity (activity per Pt mass) derived from the high specific surface area of the catalysts (surface area per Pt mass).[3−8] Because of its limited reserves and high cost, the Pt loading needs to be decreased from the present level for wider commercialization of PEFCs, and for that purpose, the mass activity of the catalysts needs to be improved.

To enhance the mass activity, substituting unused Pt atoms inside the nanoparticles with less-expensive metals is a promising method, and Pt alloys[9−16] and core−shell[17−20] catalysts have been developed. Although these catalysts were demonstrated to have specific activities higher than those of pure Pt through so-called ligand[21−23] and/or strain[24−27] effects, they were also shown to be thermodynamically unstable and easy to dissolve into acidic electrolytes under operating conditions for the cathode catalysts.[28−30] The durability of the Pt-based nanoparticles can be improved by increasing the particle size,[31−36] and some state-of-the-art Pt alloy nanoparticles give high mass activities at particle sizes larger than those of conventional ones.[15,37] Although they can potentially enhance both the activity and durability, their small specific surface area will cause another problem in the O_2 transport resistivity in catalyst layers in PEFCs, which was recently shown to increase when the catalyst surface area decreases.[38−45] Hence, it is a big challenge to improve both activity and durability without sacrificing the power density.

One strategy to resolve this trade-off problem is to utilize recently obtained atomic-scale information on the active and dissolving sites on Pt nanoparticles: (1) Edges and corners of the nanoparticles are inactive for ORR whereas facets are active, because the low-coordinated edge and corner sites are blocked strongly by adsorbed hydroxyl groups and oxygen atoms formed from water and oxygen molecules during the operations of the PEFC.[6,8,46,47] (2) Pt atoms at edges and corners are easier to dissolve into electrolytes than those at facets because those low-coordinated Pt atoms have lower dissolution potentials.[48] Thus, edges and corners of Pt nanoparticles can be regarded as useless or even harmful for the cathode catalysts of PEFCs. These observations suggest that masking or replacing Pt atoms at the edges and corners of Pt nanoparticles by inactive but stable materials can improve the durability without degrading the ORR activity similarly to the edge protections of MnO_2 oxygen evolution catalysts by TiO_2, which was recently demonstrated by Frydendal et al.[49] The concept of the edge protection for the ORR catalyst of Pt nanoparticles was proposed in theoretical studies by Wei and Liu[50] and Jinnouchi et al.,[51] where it was predicted that Au atoms preferentially segregate at edges and corners of Pt nanoparticles and that those Au atoms improve both the activity and durability.

The theoretical predictions reasonably explain experimental results reported by Zhang et al.,[52] where degradations of pure Pt nanoparticles were suppressed without significantly reducing the ORR activity by depositing Au clusters on the catalyst surfaces. In

Received: January 11, 2016
Published: March 3, 2016

DOI: 10.1021/jacs.6b00359
J. Am. Chem. Soc. 2016, 138, 4194−4200

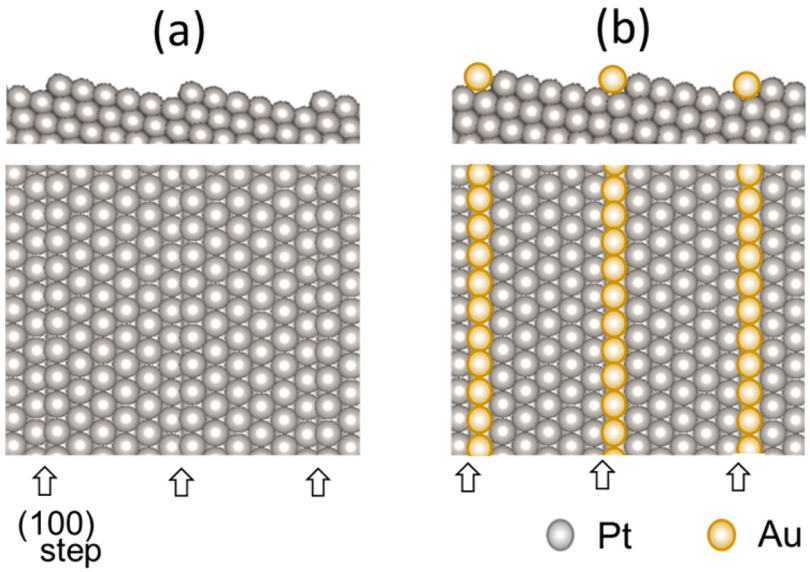

Figure 1. Side and top views of (a) a bare Pt(755) (drawn using VESTA (ver. 3))[55] and (b) the possible structure of the Au-modified Pt(755) suggested by the CV and XPS results. The positions of the (100) steps are indicated by the up-pointing arrows.

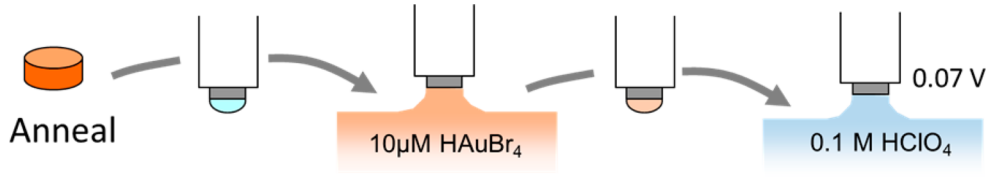

Figure 2. Schematic of the Au modification procedure.

subsequent studies by other groups,[53,54] the durability improvements of Pt nanoparticles by partially masking the surfaces with Au atoms using various methods were reported, and the results were explained with the edge-protection mechanism.[54]

Although the experimental results of the high durability seem to confirm the theoretical predictions, there is no direct evidence supporting the edge-protection concept. Difficulties to obtain the direct evidence mainly stem from the difficulty to identify locations of the deposited Au atoms on Pt nanoparticles that have uncontrolled and complex surface morphologies. In addition, remarkable enhancements in the ORR activity predicted by the theoretical calculations were not observed in those experiments.

In the present study, the theoretically predicted effects by the surface modifications with Au atoms were experimentally verified by using well-defined stepped-Pt single-crystal surfaces.

EXPERIMENTAL SECTION

The main surface tested in this study was a Pt(755) surface, which consists of (111) terraces with the width of 6 atoms separated by monoatomic (100) steps (Figure 1a),[55] also noted as Pt[6(111) × (100)]. The surface was chosen as a model of nanoparticles because its local structures at the terrace and step are the same as those at (111) facets and (111)/(100) edges on a Pt nanoparticle, and the ORR activity at this edge was predicted to be particularly low.[6] Supplemental experiments were also carried out using Pt(322) ([5(111) × (100)]), Pt(211) ([3(111) × (100)]), and Pt(332) ([5(111) × (110)]). Their ORR activities were also measured by several groups,[56−59] and our results can be cross-checked.

The electrode surface of Pt(*hkl*) was prepared by annealing a Pt single-crystal disk surfaced with a plane of (*hkl*) (99.99%, 0.196 cm^2, purchased from MaTecK) in reductive atmosphere. The prepared Pt(*hkl*) surface was modified with Au by immersing it into 10 μM $HAuBr_4$ and then moving it to 0.1 M $HClO_4$ saturated with Ar while the electrode potential was preset at 0.07 V versus the reversible hydrogen electrode (vs RHE) (Figure 2). Au atoms are expected to deposit electrochemically at the moment that the electrode surface makes a contact with the $HClO_4$ solution:

$$AuBr_4^- + 3e^- \rightarrow Au^0 + 4Br^- \quad (1)$$

for which the standard equilibrium potential is 0.91 V (vs RHE).[60] The Au complex may be also chemically reduced by metallic platinum to form platinum oxides before moving to the $HClO_4$ solution:

$$3Pt^0 + 3H_2O + AuBr_4^- \rightarrow 3Pt(OH) + 3H^+ + Au^0 + 4Br^- \quad (2)$$

This reaction is, however, not likely to be a major process in the Au depositions because the Au modification treatments were done in air atmosphere, and the Pt surfaces are expected to have been already oxidized.

The electrochemical properties were examined by taking the cyclic voltammograms (CVs) and ORR polarization curves in 0.1 M $HClO_4$ saturated with Ar and O_2, respectively, in the configuration of hanging meniscus rotating disk electrode (HM-RDE).[61] All electrode potentials are referred to RHE and corrected for ohmic drops in this article. The current densities shown below are the values obtained by normalizing the measured currents by the geometric areas of the electrodes (0.196 cm^2). The temperature was 300 K. The amount of Au on the Au-modified Pt(755) surface was estimated by X-ray photoelectron spectroscopy (XPS) after the electrochemical measurements. The details of the experimental procedure are described in the Supporting Information.

DOI: 10.1021/jacs.6b00359
J. Am. Chem. Soc. 2016, 138, 4194−4200

RESULTS AND DISCUSSION

Masking Sites of Au Atoms. Figure 3 shows the CVs for Pt(111), Pt(755), and the Au-modified Pt(755) (denoted Au/Pt(755) below). The reversible plateaus (0.05−0.4 V) and butterfly peaks (0.6−0.9 V) observed for Pt(111) are ascribed to the desorption/adsorption of underpotentially deposited hydrogen (H_{upd}) and formation/reduction of Pt hydroxide (OH(ads)), respectively.[62,63] For Pt(755), sharp peaks due to (100) steps are observed at 0.29 V as well as the plateaus for (111) terraces in the H_{upd} region.[64−66] The charge of the anodic (100) step peak (shaded area in Figure 3) is 34.7 μCcm^{-2}, which corresponds to the number density for H_{upd} atoms of 2.2×10^{14} cm^{-2}. This value is slightly lower than the geometrically calculated number density for the (100) step Pt atoms, 2.6×10^{14} cm^{-2}, probably because of the presence of defects in the (100) steps as implicated by the broad peak below 0.2 V due to (110) step sites.[67]

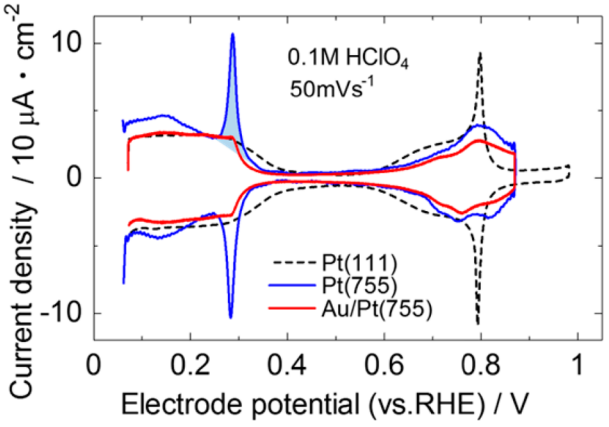

Figure 3. CVs for Pt(111), Pt(755), and the Au-modified Pt(755). The charge of the anodic (100) step peak (shaded area) is 34.7 μC cm^{-2}.

By the Au modification, the Pt(100) step peaks have disappeared, whereas the Pt(111)-terrace contribution has remained. These results suggest that Au atoms were deposited selectively at the Pt(100) step sites. Detailed comparisons indicate that the broad peaks due to (110) step defects superposed on the (111) plateaus have also disappeared, and the (111) plateaus have been flattened by the Au modification as shown in Figure 3. The changes can be ascribed to masking of the (110) step defects by the Au atoms. The selective Au-depositions at the step sites are also implicated by the behaviors in the higher potential region shown in Figure 4; the Au-deposited electrode has lost the peak at 0.92 V, which is seemingly ascribed to the oxidation of the step Pt atoms. The effects of the Au modification on the CVs of other stepped surfaces are shown in Figure S1. The results show that the Au-depositions are also step-selective on Pt(322) and Pt(211), which contain (100) steps. On Pt(332), which contains (110) steps, as shown in Figure S2, the Au depositions are less step-selective than the surfaces with (100) steps, but a detailed peak analysis indicated that the Au depositions are still preferential on the (110) step sites compared to the (111) terraces. (The Au coverage is 46% at (110) step, while it is 25% at (111) terrace.)

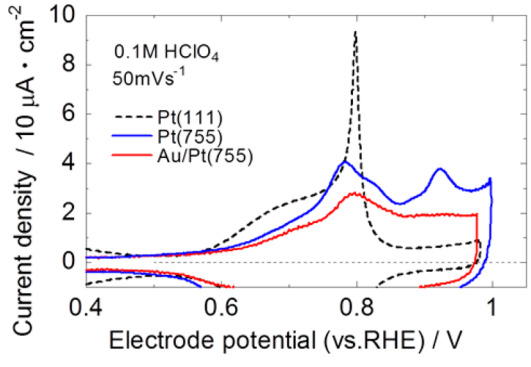

Figure 4. CVs in the potential region where Pt (hydr)oxides are formed.

The selective depositions of Au atoms on the step sites are also supported by the XPS analyses. Figure 5 shows the obtained spectra for the Au-modified Pt(755). In a wide-range spectrum (Figure 5a), small paired peaks due to Au 4f are observed between 82−90 eV in addition to large ones due to Pt 4f between 69−80 eV. The number density of Au atoms on the Pt surface, n_{Au}, can be roughly estimated from the peak areas of Au $4f_{5/2}$ and Pt 4f narrow-range spectra (Figure 5b and 5c) by taking account of the relative sensitivity factors of the peaks[68] and contribution from the bulk Pt to the XPS signal with the exponential decay characterized by the inelastic mean free path (IMFP) of the photoelectron in Pt metal[69,70] as described in the Supporting Information. The estimated n_{Au} is 1.7×10^{14} ($\pm 0.7 \times 10^{14}$) cm^{-2}, which is roughly equal to the number density for (100) step Pt atoms, 2.2×10^{14} cm^{-2} (from the H_{upd} peak). The result is reasonably explained by assuming that each Pt(100) step site has been covered by one Au atom as expected from the CV analysis.

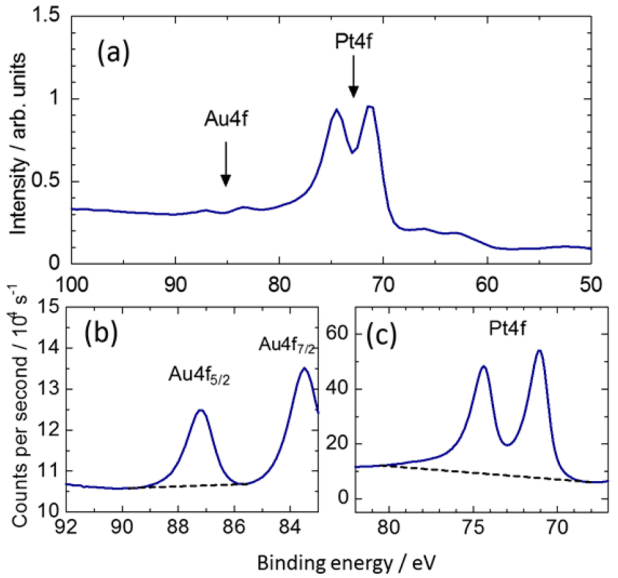

Figure 5. XPS results for the Au-modified Pt(755) (a) in a wide range, (b) in the narrow range for Au $4f_{5/2}$, and (c) in the narrow range for Pt 4f. The black dashed lines are the baselines for calculating the peak areas.

The CV and XPS analyses confirm the selective depositions of Au at the (100) step sites. Figure 1b shows a possible structure of the Au-modified Pt(755), where the Au atoms occupy 4-fold hollow sites on the (100) step.

It is an interesting question how the selective Au depositions can be accomplished by such a simple experimental procedure, where the Pt surface was merely immersed in the solution of the Au complex and then potential-cycled in an electrolyte without Au. Supplementary experiments indicate that Au atoms can be deposited even when the electrode is rinsed with pure water after

DOI: 10.1021/jacs.6b00359
J. Am. Chem. Soc. 2016, 138, 4194−4200

the immersion into the Au complex solution as shown in Figure S3. The results indicate that Au complexes are adsorbed on the electrode surfaces during the immersion, and those Au complexes are reduced to Au^0 through reaction 1 after the transfer to the $HClO_4$ solution (Figure 2). The Au adsorption itself can be preferential to the step sites, but the aligned structure can be also formed after random adsorption and reduction through fast random movements of reduced Au atoms followed by settling down of those Au atoms to the step sites, as suggested by Herrero et al.[71] in the study on bismuth deposition on stepped-Pt surfaces. In either case, Au is segregated at step edges and stabilizes the Pt surface by covering or replacing unstable low-coordinated Pt atoms with Au atoms, which have a surface energy smaller than Pt atoms as indicated by first-principles calculations.[51,72,73] Additional first-principles calculations on the cohesive energies of Au atoms on Pt(322) surface and in Au bulk summarized in Table S1 also indicate that the deposited Au atoms energetically prefer the step sites to the terrace sites or bulk agglomeration. Although preferential Au depositions on (100) step sites on Pt single-crystal surfaces were already reported by Hazzazi et al.,[74] it should be noted that the Au depositions in our study are considerably more selective to the step sites. Because their experiments employed chemical reduction of gold chloride by hydrogen for their gold deposition process, it may be important to use appropriate types of reduction methods (and gold precursors) for achieving the self-organizing Au alignment.

ORR Activity. Figure 6 shows the ORR polarization curves for Pt(111), Pt(755), and Au/Pt(755). The diffusion-limiting

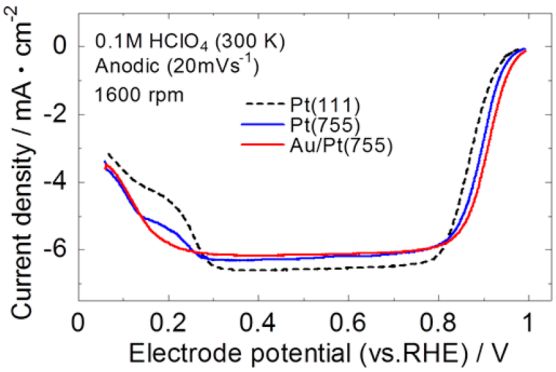

Figure 6. ORR polarization curves for Pt(111), Pt(755), and Au/Pt(755).

plateaus are clearly seen in the potential range of 0.3−0.8 V for all the electrodes, and those currents are close to the theoretical value of 6.2 mA cm^{-2}.[75] By using the well-defined diffusion-limiting current, the ORR kinetic current was obtained by the usual mass-transport correction[75] described as

$$i_k(E) = \frac{i_d\, i(E)}{i_d - i(E)} \quad (3)$$

where $i_k(E)$ is the kinetic current, i_d is the diffusion limiting current, $i(E)$ is the measured current, and E is the electrode potential.

Figure 7 shows the Tafel plots for the ORR kinetic currents. The ORR activities are in the order of Au/Pt(755) > Pt(755) > Pt(111). The ORR-improving factors at 0.9 V are 2.3 from Pt(111) to Pt(755) and 1.7 from Pt(755) to Au/Pt(755), and

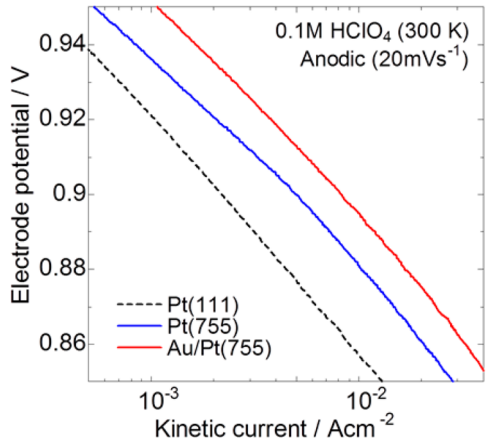

Figure 7. Tafel plots for the ORR kinetic currents on Pt(111), Pt(755), and Au/Pt(755). The current densities were obtained by normalizing the measured currents by the geometric area of the electrode (0.196 cm^2).

this result indicates that the Au modification enhances the ORR activity as the theories predicted.[50,51]

The effects of the Au modifications on the ORR activities on other stepped surfaces are shown in Figure S1. The ORR-improving effect is also observed on Pt(322) ([5(111) × (100)]) and Pt(332) ([5(111) × (110)]), whereas it is not clearly observed on Pt(211) ([3(111) × (100)]). The ORR activities at 0.9 V (vs RHE) on the bare and Au-modified Pt surfaces containing (100) steps, to which Au atoms are more selectively deposited than to (110) steps, are plotted against the number density of the steps per unit length in Figure 8. The results show volcano trends for both the series as well as the prominent improvements in the ORR activity on Pt(755) and Pt(322) by the Au modifications. The origin of the Au effects as well as the step-induced ORR-activity improvements is discussed in the following paragraphs.

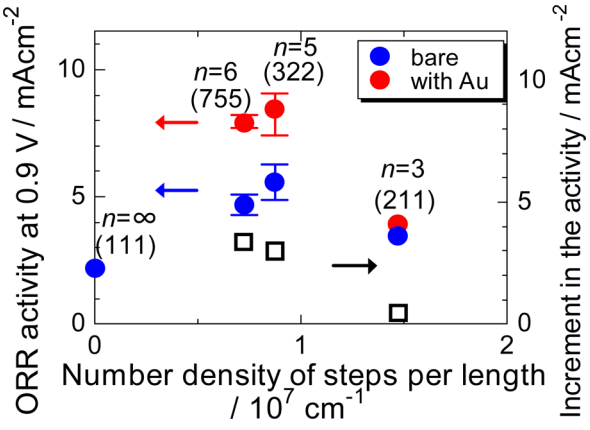

Figure 8. ORR activities at 0.9 V (vs RHE) on the bare and Au-modified Pt surfaces containing (100) steps (filled circle) and the increments in the ORR activity by the Au modifications (open square) plotted against the number density of steps per unit length. Multiple independent experiments were conducted for the surfaces where ORR improvements by the Au modifications were observed (three times each for Pt(755), Au/Pt(755), and Au/Pt(322) and twice for Pt(322)). The plot and error bars for the respective surfaces represent the averaged and maximum/minimum values of the obtained ORR activities, respectively. The number n indicates the atomic width of the (111) terrace on the electrode surface.

DOI: 10.1021/jacs.6b00359
J. Am. Chem. Soc. 2016, 138, 4194−4200

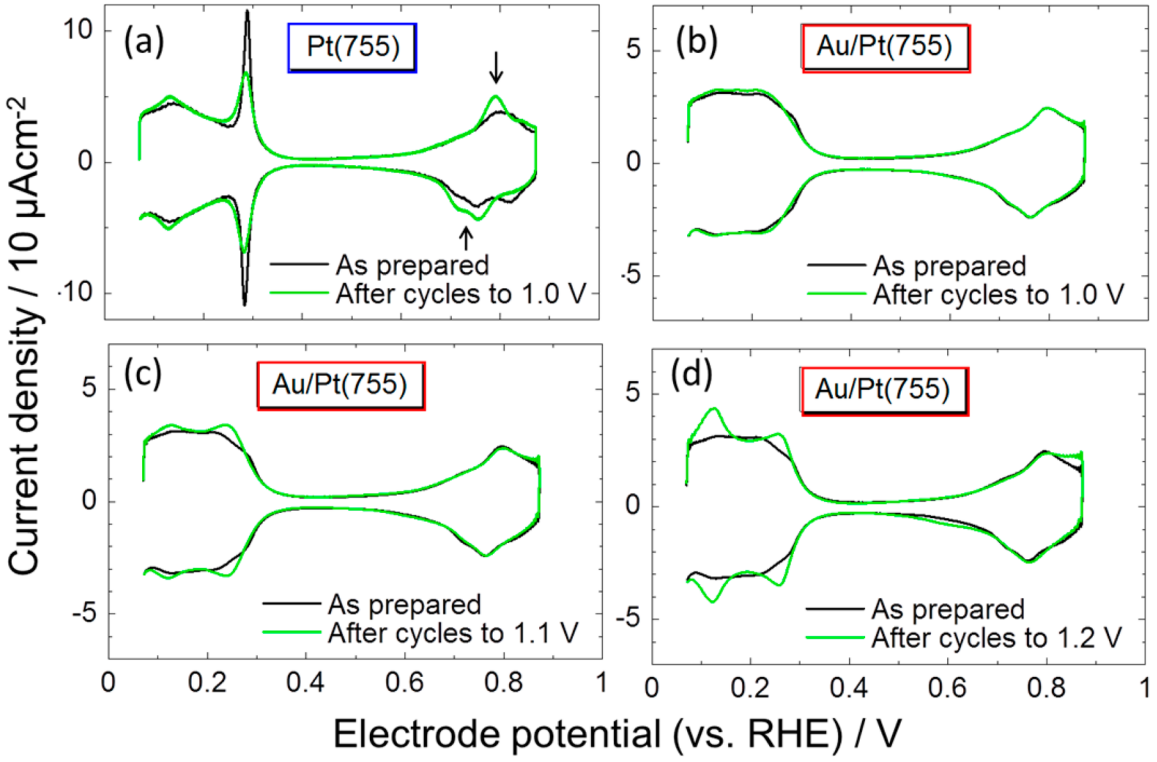

Figure 9. CVs before and after 10 potential-cycles on (a) bare Pt(755) with the upper limit (E_{upper}) of 1.0 V, (b) Au-modified Pt(755) with E_{upper} = 1.0 V, (c) Au-modified Pt(755) with E_{upper} = 1.1 V, and (d) the Au-modified Pt(755) with E_{upper} = 1.2 V. Black, before the cycles; green, after the cycles.

Bandarenka et al.[76] summarized the trend in ORR activities on stepped Pt surfaces in a volcano plot versus the OH(ads) formation potential. In the volcano plot, Pt(111) has a slightly lower OH(ads) formation potential than the optimal. Introductions of an adequate number of steps to the (111) surface can make the OH(ads) formation potential closer to the optimal; therefore, the ORR activity should increase on some stepped Pt surfaces. Too many steps, however, make the OH(ads) formation potential higher than the optimal, and on those stepped Pt surfaces, the ORR activity goes down again. The volcano trend of the ORR activity on the stepped Pt surfaces surprisingly agrees well with the volcano trend observed on (111) surfaces of Pt alloys and core−shells,[10,17,77,78] which was well-explained by the Sabatier principle proposed by Nørskov et al.,[1] where the ORR rate is limited by OH(ads) and/or O(ads) removal steps when the OH(ads) and/or O(ads) formation potentials are lower than the optimal, whereas the ORR rate is limited by the OH(ads) and/or O(ads) formation steps when the formation potentials are higher. On the basis of the agreement in the volcano plot between the stepped surfaces and (111) surfaces, Bandarenka et al.[76] suggested that the active sites of the ORR on the stepped Pt surfaces are still located on (111) terraces whereas the local ORR activity of the (111) terrace is changed by the introduction of the steps. The suggestion was recently supported by our density functional theory calculations,[79,80] which showed that both OH(ads) and O(ads) at (111) terraces are destabilized on the stepped Pt surfaces by deformations in H-bond networks surrounding them and that the destabilizations cause enhancements in the ORR activity.

In the same manner, the Au-induced ORR activity improvements can be likely ascribed to the changes in the stability of OH(ads) on Pt(111) terrace by the Au atoms at the steps. Indeed, the experimental results, in which the increase in ORR activity by the Au modification (Δi_K) was not proportional to the step density (the open squares in Figure 8), implicate that the ORR-active sites contributing to Δi_K are located not on the 1D Au atomic row at the steps but on Pt(111) terrace. The same effect is also observed on Pt(332) with (110) steps and (111) terraces, where the Au modification also improved the ORR activity as shown in Figure S1c. The result indicates that the ORR improvement is intrinsic to the (111)-terrace geometry and not due to the local step geometry ((100) step or (110) step). On either stepped surfaces, the Au atoms at the steps can affect the stability of OH(ads) at the terraces by modifying the H-bond networks surrounding OH(ads) or by making the (111)-terrace sites near the step sites available for ORR by suppressing the oxide formation near the steps as the theories indicated.[50,51] The detailed mechanisms are, however, not yet clear, and further studies are necessary for the clarification.

Stability of Surface Structure. Figure 9 summarizes the changes in the CVs on a bare Pt(755) after 10 cycles between 0.07−1.0 V and the Au-modified Pt(755) after 10 cycles between 0.07 V and 1.0, 1.1, or 1.2 V in deaerated 0.1 M $HClO_4$ at room temperature.

On bare Pt(755) (Figure 9a), the sharp peaks at 0.29 V due to H_{upd} on Pt(100) steps were attenuated, and the broad peaks below 0.2 V due to H_{upd} on Pt(110) steps were slightly developed after the potential cycles. The results are consistent with the experimental results reported by Björling et al.,[67] indicating that the unstable (100) steps disappeared and that more stable (110) steps were formed. The changes in the shape of voltammogram also appeared in the potential region of the formation of OH(ads) between 0.6−0.85 V, where the cycled electrode shows irreversible small bumps in the CV (the arrows in Figure 9a), and this change is also seemingly ascribed to the change in the surface morphology. The bare Pt(100) steps are, therefore, unstable

DOI: 10.1021/jacs.6b00359
J. Am. Chem. Soc. 2016, 138, 4194−4200

under the potential cycles between 0.07 and 1.0 V, which is in the normal operating potential range of cathode catalysts in PEFCs.

In contrast, the CV for the Au-modified Pt surface was almost completely unchanged under the potential cycles between 0.07 and 1.0 V (Figure 9b). The result indicates that the vulnerable Pt(100) step sites were protected by nobler Au atoms as the theories predicted.[50,51]

When the upper potential was raised up to 1.1 V, however, small changes were observed in the H_{upd} region of the CV on the Au-modified Pt(755) surface. As shown in Figure 9c, the (110) and (100) step peaks became slightly visible after the potential cycles. When the upper-limit potential was raised further up to 1.2 V, these changes became clearer as shown in Figure 9d. Those results suggest that Au atoms were partially detached from the steps when the upper potential was raised.

In addition to the test in the deaerated electrolyte, potential cycles were conducted in O_2-saturated electrolyte using the Au-modified Pt(322), which also contains (100) steps and showed the selective Au-depositions on the steps and higher ORR activity than the bare surface (Figure S1). The result indicates that the ORR-improving effect by the Au modification was lost once the electrode was subjected to potential cycles between 0.07 and 1.2 V as shown in Figure S5 and can be explained by assuming that the Au detaches from the Au-modified Pt(322) when the upper-limit potential is raised up to 1.2 V, similar to the case of the Au-modified Pt(755) surface in the deaerated electrolyte (Figure 9d).

In summary, Au atoms deposited selectively on the steps were shown to stabilize the (100) steps as the theories indicated.[50,51] Although the stabilization effects are limited to the potentials up to 1.0 V, the selective depositions of Au atoms on the step edges can be regarded as one of a few promising methods to suppress the catalyst degradations without decreasing the ORR activity.

CONCLUSIONS

Selective depositions of Au atoms at step sites on stepped-Pt surfaces were successfully achieved by a simple electrochemical process, and their effects on the ORR activity and stability were examined. Both the ORR activity and stability were shown to be improved by the surface Au atoms, and the theoretically predicted edge-protection concept was confirmed to work on well-defined single-crystal surfaces. Thus, the surface modification by selective Au-depositions on vulnerable sites is a promising method to enhance both the ORR activity and durability of cathode catalysts for PEFCs. The same concept and strategy can be also applied to a wide range of gas-phase and electrochemical inhomogeneous catalysts that suffer from a trade-off dilemma between the catalytic activity and durability.

ASSOCIATED CONTENT

Supporting Information

The Supporting Information is available free of charge on the ACS Publications website at DOI: 10.1021/jacs.6b00359.

Details of the experimental procedure, results of the effects of the Au modification on the CVs and ORR activities on other facets, analysis of the selectivity of the Au depositions on Pt(332), estimation of Au amount from XPS data, result of the Au modification treatment with rinsing, first-principles calculations of energetics of Au atoms on Pt(322) surfaces, and change in the ORR activity on Au-modified Pt(322) during potential cycles. (PDF)

AUTHOR INFORMATION

Corresponding Author

*kkodama@mosk.tytlabs.co.jp

Notes

The authors declare no competing financial interest.

ACKNOWLEDGMENTS

This work was financially supported by NEDO (New Energy and Industrial Technology Development Organization).

REFERENCES

(1) Nørskov, J. K.; Rossmeisl, J.; Logadottir, A.; Lindqvist, L.; Kitchin, J. R.; Bligaard, T.; Jonsson, H. *J. Phys. Chem. B* **2004**, *108*, 17886−17892.

(2) Yu, T. H.; Hofmann, T.; Sha, Y.; Merinov, B. V.; Myers, D. J.; Heske, C.; Goddard, W. A. *J. Phys. Chem. C* **2013**, *117*, 26598−26607.

(3) Gasteiger, H. A.; Kocha, S. S.; Sompalli, B.; Wagner, F. T. *Appl. Catal., B* **2005**, *56*, 9−35.

(4) Joo, S. H.; Kwon, K.; You, D. J.; Pak, C.; Chang, H.; Kim, J. M. *Electrochim. Acta* **2009**, *54*, 5746−5753.

(5) Nesselberger, M.; Ashton, S.; Meier, J. C.; Katsounaros, I.; Mayrhofer, K. J. J.; Arenz, M. *J. Am. Chem. Soc.* **2011**, *133*, 17428−17433.

(6) Shao, M. H.; Peles, A.; Shoemaker, K. *Nano Lett.* **2011**, *11*, 3714−3719.

(7) Xu, Z.; Zhang, H. M.; Zhong, H. X.; Lu, Q. H.; Wang, Y. F.; Su, D. S. *Appl. Catal., B* **2012**, *111-112*, 264−270.

(8) Perez-Alonso, F. J.; McCarthy, D. N.; Nierhoff, A.; Hernandez-Fernandez, P.; Strebel, C.; Stephens, I. E. L.; Nielsen, J. H.; Chorkendorff, I. *Angew. Chem., Int. Ed.* **2012**, *51*, 4641−4643.

(9) Toda, T.; Igarashi, H.; Watanabe, M. *J. Electrochem. Soc.* **1998**, *145*, 4185−4188.

(10) Stamenkovic, V. R.; Fowler, B.; Mun, B. S.; Wang, G. F.; Ross, P. N.; Lucas, C. A.; Markovic, N. M. *Science* **2007**, *315*, 493−497.

(11) Koh, S.; Strasser, P. *J. Am. Chem. Soc.* **2007**, *129*, 12624−12625.

(12) Cui, C. H.; Gan, L.; Li, H. H.; Yu, S. H.; Heggen, M.; Strasser, P. *Nano Lett.* **2012**, *12*, 5885−5889.

(13) Choi, S. I.; Xie, S. F.; Shao, M. H.; Odell, J. H.; Lu, N.; Peng, H. C.; Protsailo, L.; Guerrero, S.; Park, J. H.; Xia, X. H.; Wang, J. G.; Kim, M. J.; Xia, Y. N. *Nano Lett.* **2013**, *13*, 3420−3425.

(14) Chen, C.; Kang, Y. J.; Huo, Z. Y.; Zhu, Z. W.; Huang, W. Y.; Xin, H. L. L.; Snyder, J. D.; Li, D. G.; Herron, J. A.; Mavrikakis, M.; Chi, M. F.; More, K. L.; Li, Y. D.; Markovic, N. M.; Somorjai, G. A.; Yang, P. D.; Stamenkovic, V. R. *Science* **2014**, *343*, 1339−1343.

(15) Hernandez-Fernandez, P.; Masini, F.; McCarthy, D. N.; Strebel, C. E.; Friebel, D.; Deiana, D.; Malacrida, P.; Nierhoff, A.; Bodin, A.; Wise, A. M.; Nielsen, J. H.; Hansen, T. W.; Nilsson, A.; Stephens, I. E. L.; Chorkendorff, I. *Nat. Chem.* **2014**, *6*, 732−738.

(16) Huang, X. Q.; Zhao, Z. P.; Cao, L.; Chen, Y.; Zhu, E. B.; Lin, Z. Y.; Li, M. F.; Yan, A. M.; Zettl, A.; Wang, Y. M.; Duan, X. F.; Mueller, T.; Huang, Y. *Science* **2015**, *348*, 1230−1234.

(17) Zhang, J. L.; Vukmirovic, M. B.; Xu, Y.; Mavrikakis, M.; Adzic, R. R. *Angew. Chem., Int. Ed.* **2005**, *44*, 2132−2135.

(18) Zhang, J.; Lima, F. H. B.; Shao, M. H.; Sasaki, K.; Wang, J. X.; Hanson, J.; Adzic, R. R. *J. Phys. Chem. B* **2005**, *109*, 22701−22704.

(19) Zhao, X.; Chen, S.; Fang, Z. C.; Ding, J.; Sang, W.; Wang, Y. C.; Zhao, J.; Peng, Z. M.; Zeng, J. *J. Am. Chem. Soc.* **2015**, *137*, 2804−2807.

(20) Choi, S. I.; Shao, M. H.; Lu, N.; Ruditskiy, A.; Peng, H. C.; Park, J.; Guerrero, S.; Wang, J. G.; Kim, M. J.; Xia, Y. N. *ACS Nano* **2014**, *8*, 10363−10371.

(21) Tsai, H. C.; Hsieh, Y. C.; Yu, T. H.; Lee, Y. J.; Wu, Y. H.; Merinov, B. V.; Wu, P. W.; Chen, S. Y.; Adzic, R. R.; Goddard, W. A. *ACS Catal.* **2015**, *5*, 1568−1580.

(22) Lin, S. P.; Wang, K. W.; Liu, C. W.; Chen, H. S.; Wang, J. H. *J. Phys. Chem. C* **2015**, *119*, 15224−15231.

(23) Spanos, I.; Kirkensgaard, J. J. K.; Mortensen, K.; Arenz, M. *J. Power Sources* **2014**, *245*, 908−914.

DOI: 10.1021/jacs.6b00359
J. Am. Chem. Soc. 2016, 138, 4194−4200

(24) Shao, M. H.; Odell, J. H.; Peles, A.; Su, D. *Chem. Commun.* **2014**, *50*, 2173−2176.
(25) Du, M. S.; Cui, L. S.; Cao, Y.; Bard, A. J. *J. Am. Chem. Soc.* **2015**, *137*, 7397−7403.
(26) Yang, J. H.; Chen, X. J.; Yang, X. F.; Ying, J. Y. *Energy Environ. Sci.* **2012**, *5*, 8976−8981.
(27) Suzuki, S.; Onodera, T.; Kawaji, J.; Mizukami, T.; Yamaga, K. *Appl. Catal., A* **2012**, *427-428*, 92−97.
(28) Hoshi, Y.; Yoshida, T.; Nishikata, A.; Tsuru, T. *Electrochim. Acta* **2011**, *56*, 5302−5309.
(29) Dubau, L.; Lopez-Haro, M.; Castanheira, L.; Durst, J.; Chatenet, M.; Bayle-Guillemaud, P.; Guetaz, L.; Caque, N.; Rossinot, E.; Maillard, F. *Appl. Catal., B* **2013**, *142-143*, 801−808.
(30) Schuppert, A. K.; Savan, A.; Ludwig, A.; Mayrhofer, K. J. J. *Electrochim. Acta* **2014**, *144*, 332−340.
(31) Holby, E. F.; Sheng, W. C.; Shao-Horn, Y.; Morgan, D. *Energy Environ. Sci.* **2009**, *2*, 865−871.
(32) Matsutani, K.; Hayakawa, K.; Tada, T. *Platinum Met. Rev.* **2010**, *54*, 223−232.
(33) Garbarino, S.; Pereira, A.; Hamel, C.; Irissou, E.; Chaker, M.; Guay, D. *J. Phys. Chem. C* **2010**, *114*, 2980−2988.
(34) Yang, Z.; Ball, S.; Condit, D.; Gummalla, M. *J. Electrochem. Soc.* **2011**, *158*, B1439−B1445.
(35) Xu, Z.; Zhang, H. M.; Zhong, H. X.; Lu, Q. H.; Wang, Y. F.; Su, D. S. *Appl. Catal., B* **2012**, *111-112*, 264−270.
(36) Yu, K.; Groom, D. J.; Wang, X. P.; Yang, Z. W.; Gummalla, M.; Ball, S. C.; Myers, D. J.; Ferreira, P. J. *Chem. Mater.* **2014**, *26*, 5540−5548.
(37) Choi, S. I.; Xie, S. F.; Shao, M. H.; Lu, N.; Guerrero, S.; Odell, J. H.; Park, J.; Wang, J. G.; Kim, M. J.; Xia, Y. N. *ChemSusChem* **2014**, *7*, 1476−1483.
(38) Nonoyama, N.; Okazaki, S.; Weber, A. Z.; Ikogi, Y.; Yoshida, T. *J. Electrochem. Soc.* **2011**, *158*, B416−B423.
(39) Greszler, T. A.; Caulk, D.; Sinha, P. *J. Electrochem. Soc.* **2012**, *159*, F831−F840.
(40) Owejan, J. P.; Owejan, J. E.; Gu, W. B. *J. Electrochem. Soc.* **2013**, *160*, F824−F833.
(41) Fukuyama, Y.; Shiomi, T.; Kotaka, T.; Tabuchi, Y. *Electrochim. Acta* **2014**, *117*, 367−378.
(42) Weber, A. Z.; Kusoglu, A. *J. Mater. Chem. A* **2014**, *2*, 17207−17211.
(43) Liu, H.; Epting, W. K.; Litster, S. *Langmuir* **2015**, *31*, 9853−9858.
(44) Hao, L.; Moriyama, K.; Gu, W. B.; Wang, C. Y. *J. Electrochem. Soc.* **2015**, *162*, F854−F867.
(45) Choo, M. J.; Oh, K. H.; Park, J. K.; Kim, H. T. *ChemElectroChem* **2015**, *2*, 382−388.
(46) Greeley, J.; Rossmeisl, J.; Hellmann, A.; Nørskov, J. K. *Z. Phys. Chem.* **2007**, *221*, 1209−1220.
(47) Tritsaris, G. A.; Greeley, J.; Rossmeisl, J.; Nørskov, J. K. *Catal. Lett.* **2011**, *141*, 909−913.
(48) Jinnouchi, R.; Toyoda, E.; Hatanaka, T.; Morimoto, Y. *J. Phys. Chem. C* **2010**, *114*, 17557−17568.
(49) Frydendal, R.; Paoli, E. A.; Chorkendorff, I.; Rossmeisl, J.; Stephens, I. L. *Adv. Energy Mater.* **2015**, *5*, 1500991.
(50) Wei, G. F.; Liu, Z. P. *Phys. Chem. Chem. Phys.* **2013**, *15*, 18555−18561.
(51) Jinnouchi, R.; Kodama, K.; Suzuki, T.; Morimoto, Y. *Catal. Today* **2016**, *262*, 100−109.
(52) Zhang, J.; Sasaki, K.; Sutter, E.; Adzic, R. R. *Science* **2007**, *315*, 220−222.
(53) Zhang, Y.; Huang, Q. H.; Zou, Z. Q.; Yang, J. F.; Vogel, W.; Yang, H. *J. Phys. Chem. C* **2010**, *114*, 6860−6868.
(54) Takahashi, S.; Chiba, H.; Kato, T.; Endo, S.; Hayashi, T.; Todoroki, N.; Wadayama, T. *Phys. Chem. Chem. Phys.* **2015**, *17*, 18638−18644.
(55) Momma, K.; Izumi, F. *J. Appl. Crystallogr.* **2011**, *44*, 1272−1276.
(56) Macia, M. D.; Campina, J. M.; Herrero, E.; Feliu, J. M. *J. Electroanal. Chem.* **2004**, *564*, 141−150.
(57) Kuzume, A.; Herrero, E.; Feliu, J. M. *J. Electroanal. Chem.* **2007**, *599*, 333−343.
(58) Hitotsuyanagi, A.; Nakamura, M.; Hoshi, N. *Electrochim. Acta* **2012**, *82*, 512−516.
(59) Hoshi, N.; Nakamura, M.; Hitotsuyanagi, A. *Electrochim. Acta* **2013**, *112*, 899−904.
(60) Schmid, G. M. *Standard Potentials in Aqueous Solution*; Marcel Dekker: New York, 1985.
(61) Cahan, B. D.; Villullas, H. M. *J. Electroanal. Chem. Interfacial Electrochem.* **1991**, *307*, 263−268.
(62) Wakisaka, M.; Suzuki, H.; Mitsui, S.; Uchida, H.; Watanabe, M. *Langmuir* **2009**, *25*, 1897−1900.
(63) Bondarenko, A. S.; Stephens, I. E. L.; Hansen, H. A.; Perez-Alonso, F. J.; Tripkovic, V.; Johansson, T. P.; Rossmeisl, J.; Nørskov, J. K.; Chorkendorff, I. *Langmuir* **2011**, *27*, 2058−2066.
(64) Love, B.; Seto, K.; Lipkowski, J. *J. Electroanal. Chem. Interfacial Electrochem.* **1986**, *199*, 219−228.
(65) Markovic, N. M.; Marinkovic, N. S.; Adzic, R. R. *J. Electroanal. Chem. Interfacial Electrochem.* **1988**, *241*, 309−328.
(66) Gomez, R.; Feliu, J. M.; Abruna, H. D. *Langmuir* **1994**, *10*, 4315−4323.
(67) Björling, A.; Ahlberg, E.; Feliu, J. M. *Electrochem. Commun.* **2010**, *12*, 359−361.
(68) Yeh, J. J.; Lindau, I. *At. Data Nucl. Data Tables* **1985**, *32*, 1−155.
(69) Carley, A. F.; Roberts, M. W. *Proc. R. Soc. London, Ser. A* **1978**, *363*, 403−424.
(70) Tanuma, S.; Powell, C. J.; Penn, D. R. *Surf. Interface Anal.* **1988**, *11*, 577−589.
(71) Herrero, E.; Climent, V.; Feliu, J. M. *Electrochem. Commun.* **2000**, *2*, 636−640.
(72) Deng, L.; Hu, W. Y.; Deng, H. Q.; Xiao, S. F. *J. Phys. Chem. C* **2010**, *114*, 11026−11032.
(73) Yamakawa, S.; Asahi, R.; Koyama, T. *Surf. Sci.* **2014**, *622*, 65−70.
(74) Hazzazi, O. A.; Attard, G. A.; Wells, P. B.; Vidal-Iglesias, F. J.; Casadesus, M. *J. Electroanal. Chem.* **2009**, *625*, 123−130.
(75) Bard, A. J.; Faulkner, L. R. *Electrochmical methods, Fundamentals and Applications*, 2nd ed.; John Wiley & Sons: Hoboken, NJ, 2001; pp 339−341.
(76) Bandarenka, A. S.; Hansen, H. A.; Rossmeisl, J.; Stephens, I. E. L. *Phys. Chem. Chem. Phys.* **2014**, *16*, 13625−13629.
(77) Rossmeisl, J.; Nørskov, J. K. *Surf. Sci.* **2008**, *602*, 2337−2338.
(78) Stephens, I. E. L.; Bondarenko, A. S.; Perez-Alonso, F. J.; Calle-Vallejo, F.; Bech, L.; Johansson, T. P.; Jepsen, A. K.; Frydendal, R.; Knudsen, B. P.; Rossmeisl, J.; Chorkendorff, I. *J. Am. Chem. Soc.* **2011**, *133*, 5485−5491.
(79) Jinnouchi, R.; Nagoya, A.; Kodama, K.; Morimoto, Y. *J. Phys. Chem. C* **2015**, *119*, 16743−16753.
(80) Nagoya, A.; Jinnouchi, R.; Kodama, K.; Morimoto, Y. *J. Electroanal. Chem.* **2015**, *757*, 116−127.

DOI: 10.1021/jacs.6b00359
J. Am. Chem. Soc. 2016, 138, 4194−4200